

IMPACT OF LATERAL VARIATIONS ON THE SOLAR CELL EFFICIENCY

David Hinken, Karsten Bothe and Rolf Brendel

Institute for Solar Energy Research Hamelin (ISFH), Am Ohrberg 1, 31860 Emmerthal, Germany

Tel: +49 5151 999 414; Fax: +49 5151 999 400; Email: hinken@isfh.de

ABSTRACT: We propose a simple two-dimensional approach to calculate the impact of local parameters on the global solar cell efficiency. The presented local impact analysis (LIA) is based on the independent diode model. All parameters of the two-diode model can either be inserted as measured parameter mapping or as global values. To demonstrate the applicability of the presented approach we use the general-purpose circuit simulation program SPICE and simulate solar cells which suffer from high local series resistances. The results of this simulation show a good agreement to the results obtained from the local impact analysis. For the experimental demonstration we analyze various monocrystalline silicon solar cells. The light-IV curves around the maximum power point of the analyzed cells are in good agreement to the measured characteristics and indicate a good physical validity of the used parameters and model. As a result of the impact local analysis we obtain a power loss analysis of the different loss mechanism.

Keywords: Solar Cell Efficiencies, Characterisation, Local Parameters

1 INTRODUCTION

The characterization technique most often applied to solar cells is the measurement of the global IV characteristics under one-sun illumination (light-IV). The analysis of this characteristics yields fundamental solar cell parameters such as the energy conversion efficiency η , the open circuit voltage V_{oc} , the short circuit current density J_{sc} and the fill factor FF. If additionally the J_{sc} - V_{oc} characteristics is analyzed [1], parameters of the two-diode model such as the saturation current densities of the first J_{01} and second diode J_{02} , the series resistance R_{ser} and the shunt resistance R_{sh} can be extracted [2]. Table I exemplarily shows these parameters for an industrial screen-printed monocrystalline silicon solar cell (named solar cell A in the following).

The comparison of the measured parameters to the parameters expected from simulation or from previous experiments may allow to identify the efficiency-limiting parameter. Solar cell A (see Table I) seems to suffer from a high series resistance. However, the situation is often more complex and the analysis of global parameters alone is not sufficient. Solar cells are large-area devices and thus lateral variations of recombination and resistance parameters play an essential role and can affect substantially the global power conversion efficiency.

Several solar cell characterization techniques exist to characterize lateral variations of specific solar cell parameters. Among them are scanning and camera-based techniques which for example determine local effective diffusion lengths [3], local shunt resistances [4] and local series resistances [5, 6, 7, 8, 9, 10]. Based on these techniques one can localize material or process induced faults. However, the determined local values do not allow a direct and quantified insight into the impact of the local values onto

the global performance of the solar cell.

Figure 1 shows the series resistance mapping of the solar cell A. Using this image, it becomes clear that the origin of the high series resistance stems from a high contact resistance induced by an inhomogeneous firing temperature. However, it remains unclear if this high series resistance is the dominant loss mechanism for this solar cell. In other words, even though having quantitative lateral information about one parameter we have no information about its impact on the solar cell energy conversion efficiency.

To overcome this limitations, we propose a simple two-dimensional analysis to model the impact of parameter mappings on the solar cell efficiency. This *local impact analysis* (LIA), is based on a two-dimensional network of independent elements. Each local element of the network is characterized by parameters of the two diode-model and is connected to the terminals by an effective series resistance. Measured local or global parameters such as the saturation current densities of the diodes, the series resistance and the shunt resistance can be fed into LIA. As a result, LIA yields a power loss analysis of each input parameter in mW/cm^2 which allows to directly compare the magnitude of different loss mechanisms. Local parameters can be manipulated virtually and fed into LIA again to correct for unwanted lateral variations.

By means of simulations and experiments we prove the applicability of LIA for monocrystalline silicon solar cells suffering from high local series resistances. Regarding the simulations we compare results from LIA to an extended network modeling using the general-purpose circuit simulation program SPICE [11, 12]. For the experimental demonstration we analyze various monocrystalline silicon solar cells.

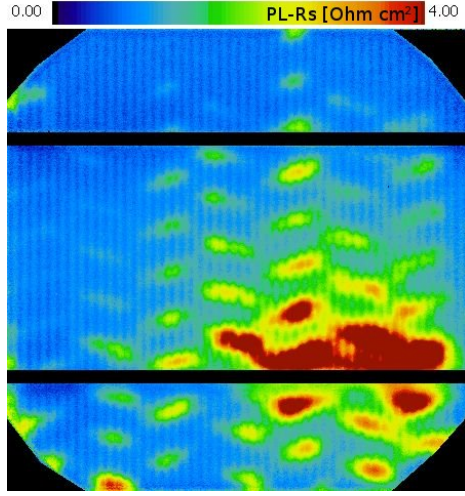


Figure 1: Series resistance image of solar cell A.

2 LOCAL IMPACT ANALYSIS

For the local impact analysis we use the model of independent diodes, shown in Fig. 2(a). The solar cell is split up laterally in many small elements which are connected with an independent series resistance to the terminals. Note that the correlation of this series resistance to the underlying emitter sheet resistance, finger resistance and busbar resistance is ambiguous since the current path of the extracted current is unknown. Thus, in the following, we refer to this series resistance as an effective local series resistance $R_{ser,i}$.

For the voltage V_{appl} , applied to the solar cell terminals, the local voltage

$$V_i = V_{appl} + R_{ser,i} \cdot I_{extr,i}. \quad (1)$$

of each element directly follows with the effective series resistance. Here, $I_{extr,i}$ gives the local current which can be extracted from element i .

In the following we use the two-diode model shown in Fig. 2(b) for parameterizing the local characteristics of a local element i . This model includes a local saturation current density $J_{01,i}$ of the first diode

Table I: Parameters extracted from the light-IV and J_{sc} - V_{oc} characteristic of solar cell A.

parameter	value
η	16.8 %
J_{sc}	35.5 mA/cm ²
V_{oc}	627 mV
FF	75.3 %
Pseudo-FF	80.6 %
Rs-FF	1.15 Ω cm ²
J_{01}	1000 fA/cm ²
J_{02}	24000 pA/cm ²
R_{sh}	4000 Ω cm ²

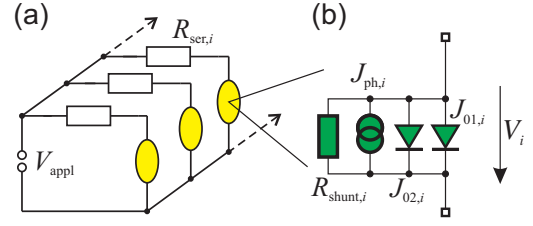


Figure 2: Model of independent diodes (a) and the equivalent circuit of one local element i (b).

describing the emitter, the base and the rear surface recombination, a local second diode current density $J_{02,i}$ which considers defects within the space charge region and a local shunt resistance $R_{sh,i}$ in parallel to the diodes. A local photo current $I_{ph,i}$ accounts for the generation of excess carriers due to the absorption of photons within the solar cell base and is the maximum extractable current of that specific region.

The local voltage V_i is the voltage of the local element and fully describes the current losses

$$I_{rec,i}(V_i) = A_{loc} J_{01,i} \exp\left(\frac{V_i}{V_T}\right) + A_{loc} J_{02,i} \exp\left(\frac{V_i}{2V_T}\right) + A_{loc} \frac{V_i}{R_{sh,i}} \quad (2)$$

within the local element, where A_{loc} is the size of the local element. The current

$$I_{extr,i}(V_i) = I_{ph,i} - I_{rec,i} \quad (3)$$

is extracted from the local element i .

Within the model of independent diodes all locally extracted currents $I_{extr,i}$ add up to the globally extracted current

$$I_{extr}(V_{appl}) = \sum_i I_{extr,i}(V_{appl}). \quad (4)$$

As a consistency check, the light-IV characteristics of LIA can be compared to the measured light-IV characteristics. If around the maximum power point both IV characteristics are in good agreement a power loss analysis can be applied to the data.

The power losses at the shunt resistance, at the series resistance and at the first and second diode of each local element, respectively, are obtained according to

$$P_{sh} = \sum_i V_i^2 / R_{sh,i}, \quad (5)$$

$$P_{ser} = \sum_i (V_{appl} - V_i)^2 / R_{ser,i}, \quad (6)$$

$$P_{J01} = \sum_i V_i \cdot J_{01,i} \exp(V_i / V_T), \quad (7)$$

$$P_{J02} = \sum_i V_i \cdot J_{02,i} \exp(V_i / 2V_T). \quad (8)$$

3 TECHNICAL IMPLEMENTATION

To carry out the calculations as indicated in Eq. (4), all parameters which are available as mappings have to be matched by means of scaling, rotation and translation. Note that A_{loc} is limited by the measurement technique having the lowest resolution.

Since Eq. (2) is given implicitly for V_{appl} we apply Newton-Raphson's method. Already after a few iterations a value for the local current $I_{extr,i}(V_{appl})$ follows with a very high precision. As indicated in Eq. (4) we add up all local currents to the global current and thus obtain one IV data pair.

Sufficient IV data pairs around the maximum power point voltage are calculated. Note that we only analyze voltages around the maximum power point voltage. For a reliable LIA calculations all measured parameters have to correspond to the injection conditions at the maximum power point.

The resulting light-IV characteristics from LIA has to be compared to the experimentally measured light-IV characteristics around the maximum power point voltage.

We take a good agreement of the model data with the experimental data as an indication for:

- the physical validity of the used parameters and
- the applicability of the model of independent diodes.

4 PARAMETER DETERMINATION

The presented analysis can be performed with all parameters given as local parameters in a parameter mapping. In this work, we analyze industrial monocrystalline silicon solar cells which suffer from high local series resistance. In this case, a parameter mapping of the effective series resistance $R_{ser,i}$ is of interest, for all other parameters global parameters are sufficient.

4.1 Series resistance mapping

All luminescence-based series resistance methods introduced so far are based on the determination of the local voltage. They use the independent diode model to determine a resistance accounting for the voltage drop from the terminals to the local region and the locally extracted current. It thus gives exactly the effective series resistance $R_{ser,i}$ introduced in the previous section.

For the determination of the local series resistance of multicrystalline silicon solar cells we prefer photoluminescence (PL) based methods [6, 9, 10] because they are able to separate $R_{ser,i}$ and $J_{0,i}$ [13, 10]. It can be shown analytically for all introduced methods based on electroluminescence (EL) imaging so far [8, 14, 15] that these methods do only determine the product $R_{ser,i} \cdot J_{0,i}$.

Fuyuki's assumption [16] was used in Ref. 14 and 15 to separate $R_{ser,i}$ and $J_{0,i}$. However, this assumption is not applicable to most industrial solar cells because it only holds for solar cells with effective diffusion lengths much smaller than the thickness of the device.

4.2 Light-IV characteristics

From the light-IV characteristics we determine the short circuit current density J_{sc} which in good approximation equals the photo current density J_{ph} for moderate series resistance. For monocrystalline solar cells the assumption holds that the local photo current density $J_{ph,i}$ equals the global photo current density J_{ph} .

4.3 $J_{sc}V_{oc}$ characteristics

The $J_{sc}-V_{oc}$ -characteristics is used to determine the saturation current densities of the first and the second diodes and the shunt resistance. Since the $J_{sc}-V_{oc}$ -characteristics is not affected by series resistances the fit of the two-diode model results in physically realistic values for standard industrial solar cells. We again use the assumption that the local recombination properties equal the global recombination properties because investigating monocrystalline silicon solar cells.

5 LIA VERSUS SPICE

We prepare an electrical network simulation similar to the ones presented in e.g. Ref. 17 and 13 to further analyze if the approximation of the independent local diode model holds around the maximum power point. We use the general-purpose circuit simulation program SPICE [11, 12] to simulate one symmetry element of a solar cell. We focus on a monocrystalline solar cell which suffers from a high local series resistance due to a broken finger. For the simulation, we cut the finger at a specific distance from the busbar. By varying this distance, the solar cell suffers globally and locally from different series resistance values. Table II summarizes all parameters inserted into the simulation.

The simulation is carried out for different applied voltages and illumination intensities to obtain the light-IV and the $J_{sc}-V_{oc}$ characteristics. At the maximum power point we extract a series resistance image as it would be extracted from a luminescence image using the approach of Trupke et al. [6]. The local and global parameters needed for LIA are determined from this data as explained in the previous section.

Figure 3 shows the results of SPICE and LIA. The x-axis gives the efficiency which is directly obtained from SPICE and the y-axis gives the value obtained from LIA. It can be seen, that both meth-

Table II: SPICE simulation parameters.

parameter	value
Illuminated base width	31 mm
Illuminated base height	1.36 mm
Resolution x	1 mm
Resolution y	0.08 mm
Half finger width	80 μm
Half busbar width	1000 μm
Busbar & Finger height	12.5 μm
Specific finger and busbar resistance	$3 \times 10^{-6} \Omega\text{cm}$
Contact resistance to emitter	$0.003 \Omega\text{cm}^2$
Emitter sheet resistance	50 Ω/sq
Shunt resistance	$1 \times 10^{10} \Omega\text{cm}^2$
Specific base resistance	1.5 Ωcm
$J_{01,i}$	1000 fA/cm^2
$J_{02,i}$	0 fA/cm^2
$J_{\text{ph},i}$	36 mA/cm^2

ods are in good agreement for the analyzed range of series resistances.

For the highest global series resistance value of $R_{\text{ser,FF}} = 2.3 \Omega\text{cm}^2$ Fig. 4 shows the light-IV and in the inset the shifted light-IV curve in a logarithmic scaling. It can be seen, that LIA is in good agreement with the light-IV curve directly obtained with SPICE. Note that the global one or two-diode model is not able to reproduce the recombination properties and would thus lead to wrong conclusions.

6 MEASUREMENTS

We analyze seven monocrystalline silicon solar cells which suffer from locally high series resistances. We carry out light-IV, $J_{\text{sc}}-V_{\text{oc}}$ and PL-Rs measurements [6] and compare the solar cell efficiency which follows directly from the light-IV characteristics to the efficiency which follows from LIA. The local and global parameters needed for LIA are determined from this data as explained in the previous section.

The result of this comparison is shown in Fig. 5. For the investigated solar cells the measured efficiencies equal the values obtained with LIA.

We carry out the loss analysis for the solar cell A, which was already introduced in Tab. I and in Fig. 1. The resulting power loss analysis is shown in Fig. 6. Obviously the locally increased series resistance leads to the most important power reduction of $1.22 \text{ mW}/\text{cm}^2$. For any improvement of the efficiency of this solar cell the series resistance is the most important parameter to work on.

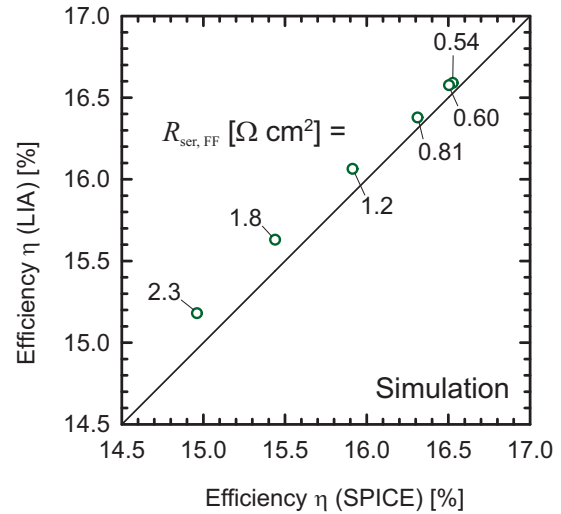


Figure 3: Simulation carried out with SPICE to demonstrate the LIA approach. The x-axis gives the efficiency obtained from SPICE and the y-axis the efficiencies calculated with LIA. For LIA we used a series resistance image and parameters determined from the light-IV and the $J_{\text{sc}}-V_{\text{oc}}$ characteristics.

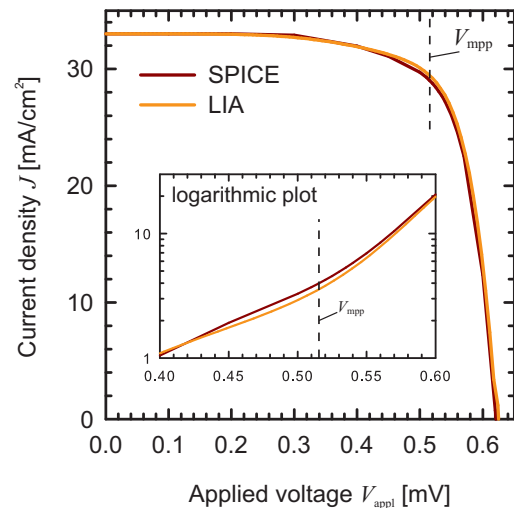


Figure 4: Light-IV curves of a symmetry element with LIA and SPICE. The inset shows the data around the maximum power point in a logarithmic scaling.

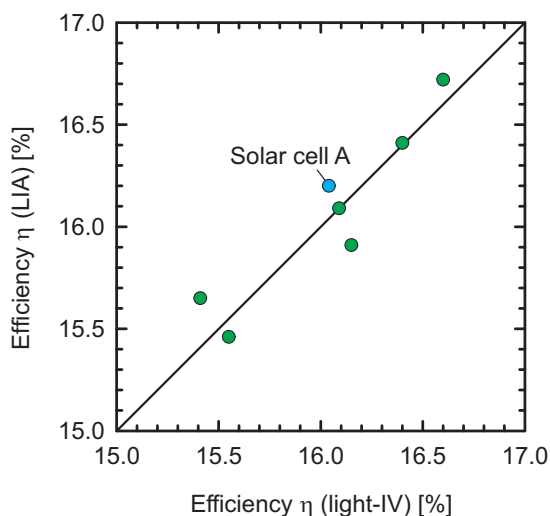


Figure 5: Comparison of efficiencies obtained from the light-IV characteristics to efficiencies calculated using the approach presented in this work. The series resistance image of solar cell A is shown in Fig. 1.

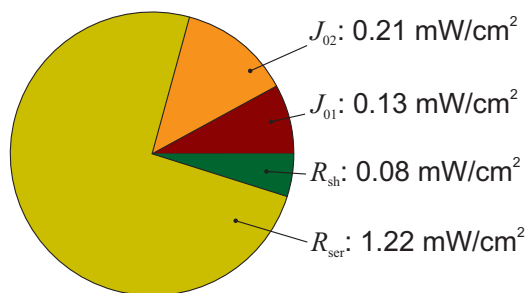


Figure 6: Power loss analysis of solar cell A. The series resistance image of this solar cell is shown in Fig. 1.

We virtually manipulate the series resistance mapping to the expected value of $0.7 \Omega\text{cm}^2$. The data is fed into LIA again and we obtain for this manipulated set of parameters a new efficiency of 17.2 %.

7 CONCLUSIONS

In this work, we proposed a simple local impact analysis to calculate the impact of local parameters onto the global solar cell efficiency. Measured parameter mappings can be fed into this approach easily and computation time is fairly low. The analysis is based on the independent diode model which was verified for solar cells with high local series resistances by simulations and experiment. As a result of the local impact analysis we obtained a power loss analysis of different loss mechanism.

ACKNOWLEDGMENTS

This work was funded by the Federal Ministry for the Environment, Nature Conservation and Nuclear Safety under contract number 0327661.

REFERENCES

- [1] M. Wolf and H. Rauschenbach, *Advanced Energy Conversion* **3**, 455 (1963).
- [2] O. Kunz, R. Brüggemann, A. Sproul, and A. Aberle, in *Proceedings of the 20th European Photovoltaic Solar Energy Conference, Barcelona, Spain* (WIP Munich, 2005).
- [3] W. Warta, J. Sutter, B. Wagner, and R. Schindler, in *Proceedings of the 2nd World Conference and Exhibition on Photovoltaic Solar Energy Conversion, Vienna, Austria* (EC Joint Research Center, Ispra, 1998), pp. 1650–1653.
- [4] O. Breitenstein, J. Rakotoniaina, M. A. Rifai, and M. Werner, *Prog. Photovolt.* **12**, 529 (2004).
- [5] J. Carstensen, G. Popkirov, J. Bahr, and H. Föll, *Sol. Energy Mater. Sol. Cells* **76**, 599 (2003).
- [6] T. Trupke, E. Pink, R. Bardos, and M. Abbott, *Applied Physics Letters* **90**, 093506 (2007).
- [7] K. Ramspeck, K. Bothe, D. Hinken, B. Fischer, J. Schmidt, and R. Brendel, *Applied Physics Letters* **90**, 153502 (2007).
- [8] D. Hinken, K. Ramspeck, K. Bothe, B. Fischer, and R. Brendel, *Applied Physics Letters* **91**, 182104 (2007).
- [9] H. Kampwerth, T. Trupke, J. W. Weber, and Y. Augarten, *Applied Physics Letters* **93**, 202102 (pages 3) (2008), URL <http://link.aip.org/link/?APL/93/202102/1>.
- [10] M. Glatthaar, J. Haunschild, M. Kasemann, J. Giesecke, W. Warta, and S. Rein, *Phys. Status Solidi RRL* **4**, 13 (2010).
- [11] J. Rabaey, *The spice home page*, EECS Department of the University of California at Berkeley (2010), URL <http://bwrc.eecs.berkeley.edu/classes/icbook/spice/>.
- [12] P. Nenzi, *Ngspice circuit simulator* (2010), URL <http://ngspice.sourceforge.net/>.
- [13] B. Michl, M. Kasemann, J. Giesecke, M. Glatthaar, A. Schütt, J. Carstensen, H. Föll, S. Rein, W. Warta, and H. Nagel, in *Proceedings of the 23rd European Photovoltaic Solar*

Energy Conference, Valencia, Spain (WIP, Munich, 2008), pp. 1176–1182.

- [14] J. Haunschild, M. Glatthaar, M. Kasemann, S. Rein, and E. Weber, *Phys. Status Solidi RRL* **3**, 227 (2009).
- [15] O. Breitenstein, A. Khanna, Y. Augarten, J. Bauer, J. Wagner, and K. Iwig, *Phys. Status Solidi RRL* **4**, 7 (2010).
- [16] T. Fuyuki, H. Kondo, Y. Kaji, T. Yamazaki, Y. Takahashi, and Y. Uraoka, in *Proceedings of the 31st Photovoltaic Specialists Conference, Lake Buena Vista, FL* (IEEE, New York, 2005), pp. 1343–1345.
- [17] D. Grote, M. Kasemann, M. Hermle, and W. Warta, in *Proceedings of the 22nd European Photovoltaic Solar Energy Conference, Milan, Italy* (2007), pp. 305–310.